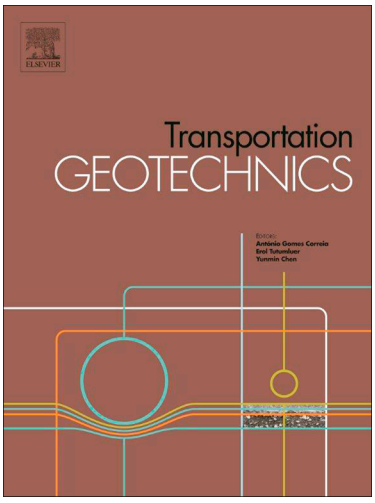

Effect of intrinsic microscopic properties and suction on swell characteristics of compacted expansive clays

E.U. Eyo, S. Ng'ambi, S.J. Abbey

PII: S2214-3912(18)30184-3
DOI: https://doi.org/10.1016/j.trgeo.2018.11.007
Reference: TRGEO 215

To appear in: *Transportation Geotechnics*

Received Date: 20 August 2018
Revised Date: 22 November 2018
Accepted Date: 24 November 2018

Please cite this article as: E.U. Eyo, S. Ng'ambi, S.J. Abbey, Effect of intrinsic microscopic properties and suction on swell characteristics of compacted expansive clays, *Transportation Geotechnics* (2018), doi: https://doi.org/10.1016/j.trgeo.2018.11.007

Revised with marked changes

Effect of intrinsic microscopic properties and suction on swell characteristics of compacted expansive clays

Eyo E. U.[a]*, Ng'ambi S.[a], Abbey S. J.[b]

(*Corresponding author Email: eyoe@coventry.ac.uk)

[a]*School of Energy, Construction and Environment, Faculty of Engineering, Environment and Computing, Coventry University, Coventry, United Kingdom.*

[b]*Faculty of Environment and Technology, Department of Geography and Environmental Management, Civil Engineering Cluster, University of the West of England.*

Abstract

The complex swelling mechanism in expansive clays during moisture ingress can be succinctly explained by an examination of their core mineralogy, microfabric, grain size and suction response. This note has attempted to investigate these influential factors on five different expansive clay samples to enable further understanding of swell behaviour. Laser diffractometry tests were performed on the expansive clays to determine the clay-sized particle structure (<2μm). One-dimensional vertical swell and swell pressure tests were carried out using the standard oedometer to establish the extent of swell. The filter paper technique was adopted to determine the matric suction values for the compacted samples. Pore sizes of the expansive clays were analytically derived and utilized to describe the swell characteristics of the clays. Further microstructural studies were conducted using the scanning electron micrograph (SEM) to better understand the pore and aggregate structure of the samples. Results of analysis of one-dimensional swell under inundation revealed an increase in swelling with increase in the montmorillonite content in the expansive clays. Swell behavioural concepts formulated to describe and predict the volume change characteristics of the clays by accounting for the clay-particle size, pore morphology and suction showed estimates of coefficient of determination exceeding 0.90 hence buttressing the critical significance of the intrinsic properties considered. This approach was tested and validated against a previous model which considered the micro-internal factors influencing swell. Very satisfactory relationships were also achieved between the inherent expansive clay properties such as plasticity index, clay activity and specific surface area.

Keywords

Expansive clays; swell potential; suction; particle size analysis; pore size.

Introduction

Expansive soils have continued to throw up vital challenges to geotechnical engineers and soil mechanics practitioners due to their undesirable swelling and shrinkage characteristics. Both man-made and periodic environmental factors work to trigger expansive soil's intrinsic mineral property with a resultant increase or decrease in the soil's volume [1]. The extensive geology of these soils the world over has made them become practically unavoidable especially in areas where their deposits are very huge [2]. Expansive soils are very problematic and almost impossible to compact during construction except after treatment with cementitious by-product materials and or recycled wastes [3–6]. The recognition and evaluation of expansive soil's capacity to swell is therefore very imperative for the achievement of a safe and secure foundation for highways and other vital land developments. Several direct and indirect methods have been developed and proposed for the prediction and estimation of the swelling capacity of expansive soils [7–12]. A vast majority of the correlations used in these past studies relied heavily on empirical relationships of some basic soil index properties such as moisture content, liquid limits, plasticity indices, etc to predict the swell strain or swell potential of expansive soils. However, it has been proven that soils having the same index properties in most instances could react or perform very differently as a result of some of their mineral composition and placement conditions such as suction, moisture content and internal voids [13]. Moreover, most of the other methods relying on chemical, mechanical and semi-empirical models to describe and evaluate expansive soil's complex swelling mechanism could be very time consuming, expensive and cumbersome to carryout [13–21]. In view of this, the current research has attempted to present a comprehensive volume change concept to enable further understanding of swell behaviour of expansive soils by incorporating the effect of clay particle sizes in relation to specific surface area (SSA) and soil activity, pore voids and suction. Apart from providing an approach that in most parts aids to circumvent some of the stressful experimental work, this study ensured a much more rational means of characterising expansive soils.

Materials and Methods

The materials used in this study consisted of a high swelling capacity clay (Sodium-montmorillonite rich bentonite) and a low swelling capacity type of Kaolin clay sourced commercially from Mistral Industrial Chemicals in Northern Ireland, United Kingdom. This choice of materials was to enable remoulding and simulation of artificially made soils with engineering properties representing those of some naturally occurring clays [22]. Therefore, the Sodium-Bentonite (SB) and Kaolin clay (CK) were mixed in five different combination ratios (0:100, 10:90, 25:75, 50:50 and 75:25 in %) by weight of dry Bentonite to form five artificially synthesized clays of varying plasticity (Soil 1 to Soil 5) as shown in Table 1. The adopted clay combination ratios were selected to achieve clay samples with broad ranging engineering properties due to variation in their chemical compositions [23] as shown in Table 2.

Revised with marked changes

Table 1
Designation of the representative expansive clays and characterisation.

Property	SB: CK (Percent by Wt.) (%)				
	SB0:CK100	SB10:CK90	SB25:CK75	SB50:CK50	SB75:CK25
	Soil 1	Soil 2	Soil 3	Soil 4	Soil 5
Liquid Limit	58	85	130	222	285
Plastic Limit	30	37	48	58	72
Plasticity Index	28	48	82	164	213
Specific Gravity	2.60	2.65	2.69	2.70	2.76
Silt Content (%)	74	70	65	58	48
Clay Content (%)	26	30	35	42	52
MDD (kN/m^3)	15.0	13.9	13.5	13.2	12.9
OMC (%)	17	21	23	25	30
Modified Activity	0.67	1.92	2.73	2.76	4.06
USCS Classification	CL	CH	CH	CH	CH

Table 2
Chemical composition of materials (Imerys minerals).

Oxide	Clay Minerals (%)	
	Bentonite	Kaolinite
SiO_2	57.1	49
Al_2O_3	17.79	36
Fe_2O_3	4.64	0.75
CaO	3.98	0.06
MgO	3.68	0.30
Na_2O	3.27	0.10
K2O	0.9	1.85
TiO_2	0.77	0.02
Mn_2O_3	0.06	-
LOI	7.85	12.0

Laboratory testing

All five clay samples were subjected to Atterberg limits test following the procedure outlined in (ASTM D 4318-17), the specific gravity test (ASTM D 854-10) and compaction test (ASTM D 698-12).

Laser Diffractometry

Grain size distribution (GSD) test was performed using the Malvern Mastersizer 2000 which operates the Hydro 2000G module of sample dispersion based on laser diffraction technology for soil particle sizing. The Mastersizer 2000 is capable of analysing particles in the range of 0.02µm to 2000µm and eliminates the sedimentation method's susceptibility to inadequate dispersion of sample and fluctuations in suspension fluid viscosity. During measurement, particles passing through a focused laser beam scatter light at an angle that is inversely

proportional to their size [24]. A series of photosensitive detectors then measures the scattered light's angular intensity. Following this, the map showing the scattering intensity versus angle becomes the primary source of information for calculating the particle size [24]. In this study, the wet method of sample dispersion was used. All five clay soils in their powdered form were first dispersed into a non-reactive liquid and then fed into the system for analysis. After the analysis, parameters such as particle D-sizes were determined from a grain size distribution and statistics (GRADISTAT) spreadsheet program [25].

Suction characteristics

The filter paper method of suction measurement (ASTM D-5298) was used in the present study to measure the matric suctions of the specimens through the contact method. The soil samples used were compacted at optimum conditions according to (ASTM D 698-12). Matric suction values were obtained from the filter paper moisture content after a minimum equilibrium period of 7 days through the calibration method [26] as given in Eqs. 1 & 2 for the Whatman 42 filter paper.

$$\varphi = 10^{2.909 - 0.0229 w_f} \qquad w_f \geq 47 \qquad \text{Eq. 1}$$

$$\varphi = 10^{4.945 - 0.0673 w_f} \qquad w_f < 47 \qquad \text{Eq.2}$$

Where:

φ = suction

w_f = filter paper water content

The air entry suction values (AEV) were determined analytically from the capillary model assuming the soil particles are spheres of uniform sizes [27]. The air entry point into a spherical arrangement of particles exists whenever the largest size-pore allows the displacement of the water within it by the air. Hence, the air-entry suction value is a function of the biggest pore opening within the particles. It is thought that the largest pore in a system of closely packed similar-size spherical particles occurs in a cubical arrangement (Fig. 1). As a result, a right-angled triangle is created by a locus through the centre between the contact points of two spheres to the midpoint of the inner capillary circle. A geometric relationship then ensues between the radius of the capillary circle and the particle spheres as in (Eq. 3). The suction across a 3-D surface is described by using the Laplace capillary equation (Eq. 4). The air-entry suction value expression (Eq. 5) is calculated by substituting Eq. 3 into Eq. 4. The mean size diameter of a spherical soil particle in a given sample shall be used in Eq. 5 to determine the AEV.

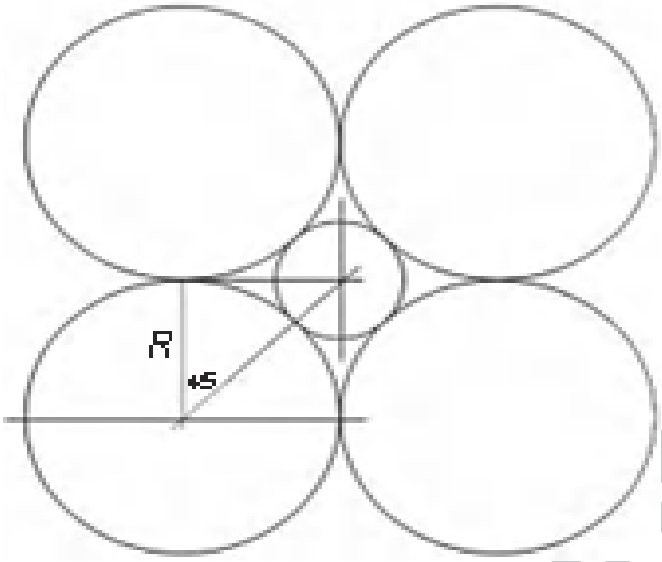

Fig. 1. Cubic layer particles arrangement used to estimate air-entry value suction [28]

$$\frac{r}{R} = arccos45° - 1 \qquad \text{Eq. 3}$$

$$u_a - u_w = \frac{4Tcos\alpha}{R} \qquad \text{Eq. 4}$$

$$u_a - u_w = \frac{0.3513}{R} \qquad \text{Eq. 5}$$

Where:

r = spherical particle radius
R = pore opening radius (mm)
T_s = surface tension of water=72.75 × 10^{-3} (N/m)
α = contact angle of water-solid interface (assumed as zero)
$u_a - u_w$ = soil matric suction

Scanning Electron Microscopy (SEM)

SEM utilizing the JOEL 6060LV in secondary mode was conducted to examine the arrangement of the voids and orientation of specimens used. Samples compacted based on (ASTM D 698-12) to ensure homogeneity and uniformity at optimum water content and maximum dry density, were cut into small sections, dried and then glued to mounting stubs using carbon cement or carbon tape and the micrographs taken.

One-dimensional oedometer test

One dimensional swell strain and swell pressure tests were performed on compacted samples using a conventional oedometer with ring dimensions 20 mm thickness and 76 mm diameter and a seating load of 5kpa in accordance to the (ASTM D-4546). The test setup was gradually inundated with water and the samples allowed to undergo vertical displacement for a minimum period of 24 hrs. The swell potential was calculated as the ratio of the increase in specimen height (H) to the original height (H), expressed as a percentage (S%) [29].

Following complete swelling of the samples, the load back method of swell pressure test was conducted on the specimens. The samples were gradually consolidated under increasing vertical loads until the initial void ratio (e_o) of each of the sample was achieved. The total pressure required to bring back the specimens to their original void ratio was used to determine the swell pressure [30].

Results and discussion

Oedometer swell description

Results of changes in vertical swell strains are shown in Fig. 2. It can be seen that the expansive clays exhibiting maximum swelling strains also gave higher swelling pressures and reduced permeability as also clearly demonstrated in Fig. 3. This is due to the presence of high quantities of montmorillonite content in the expansive clays. Vertical swell strains reached their stable peak within approximately 2, 8, 24, 50 and 333hrs with the increase in montmorillonite content of 0%, 10%, 25%, 50% and 75% respectively. The numbers attached at the end of each curve in Fig. 3 are the final void ratio values corresponding to the maximum swell potential values. The increase in the amount of montmorillonite provides the impetus for the increase in the volume of the micropores during the swelling process. This phenomenon may also be explained from the theory that the higher the quantity of montmorillonite, the more uniform the pore distribution and hence the higher the swelling potential [17]. Moreover, it could also be observed that mixtures with higher percentage content of montmorillonite took longer to swell compared to the compacted clay samples having lower quantities of montmorillonite. This is due to the small permeability and high-water retention capacity of the samples rich in montmorillonite resulting in slow water infiltration rate in the samples thus requiring relatively more time to reach the equilibrium swelling stage. Further description of the complexities of this swell behaviour are given in the subsequent sections.

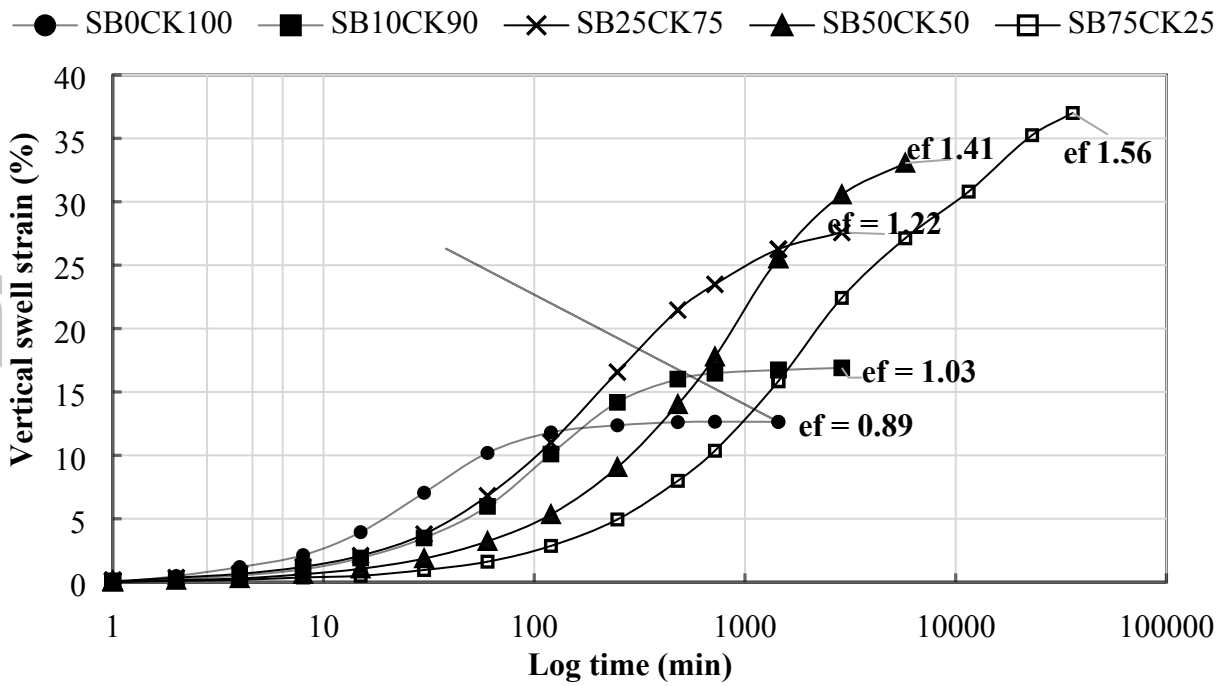

Fig. 2. Vertical swell strain versus time.

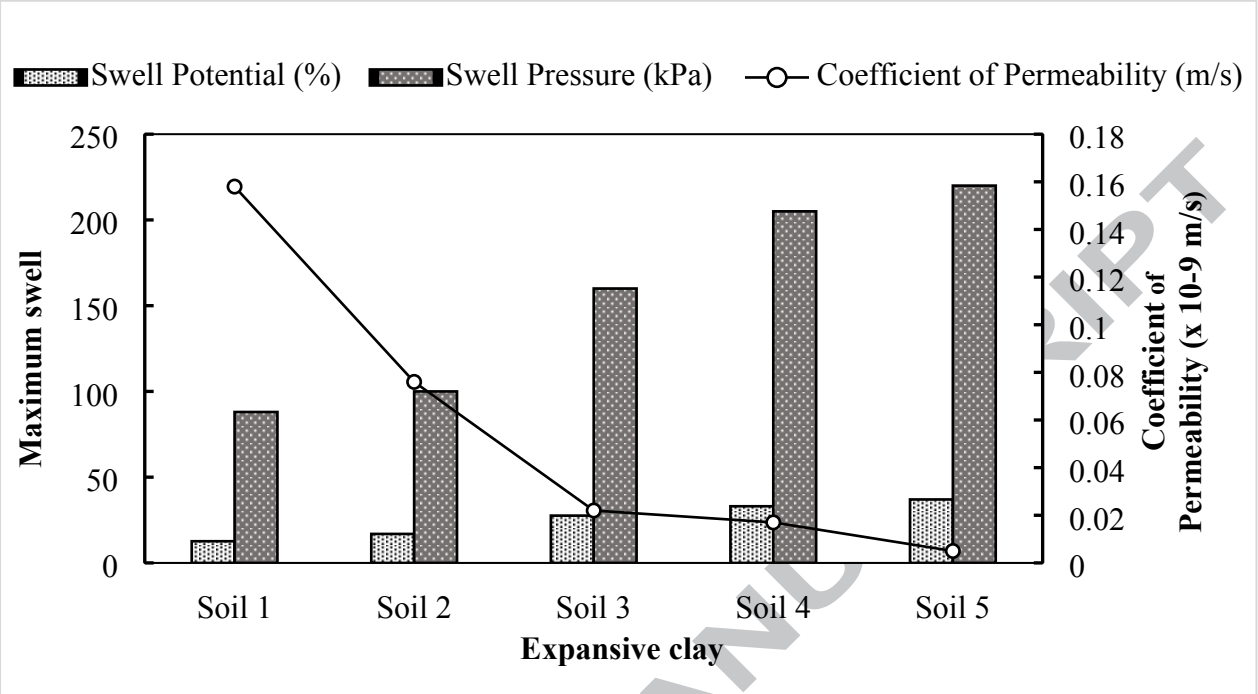

Fig. 3. Variation of maximum swell characteristics with soil type.

Microstructural analysis

SEM

Fig. 4 shows the micrographs of the compacted samples revealing their pore and aggregate. These micrographs confirm that the microfabric of Na-montmorillonite rich clays are likely to be characterised by dispersed and undulating filmy particles as compared to the low swelling kaolin rich china clay with more of a leaf-like arrangement [31]. As the montmorillonite content increases, the compacted mixtures tend to exhibit aggregated and concentrated clusters of clay particles. This behaviour gives rise to impervious layers thus resulting in initial low swelling rate at the primary swelling stage but with the ultimate free swelling under inundation taking a longer time to be completed. This phenomenon also invariably suggests that as the kaolin content increases, the pore structure become more interlinked resulting in high permeability rate at the initial and primary stages and reduced time of swelling when inundated.

Revised with marked changes

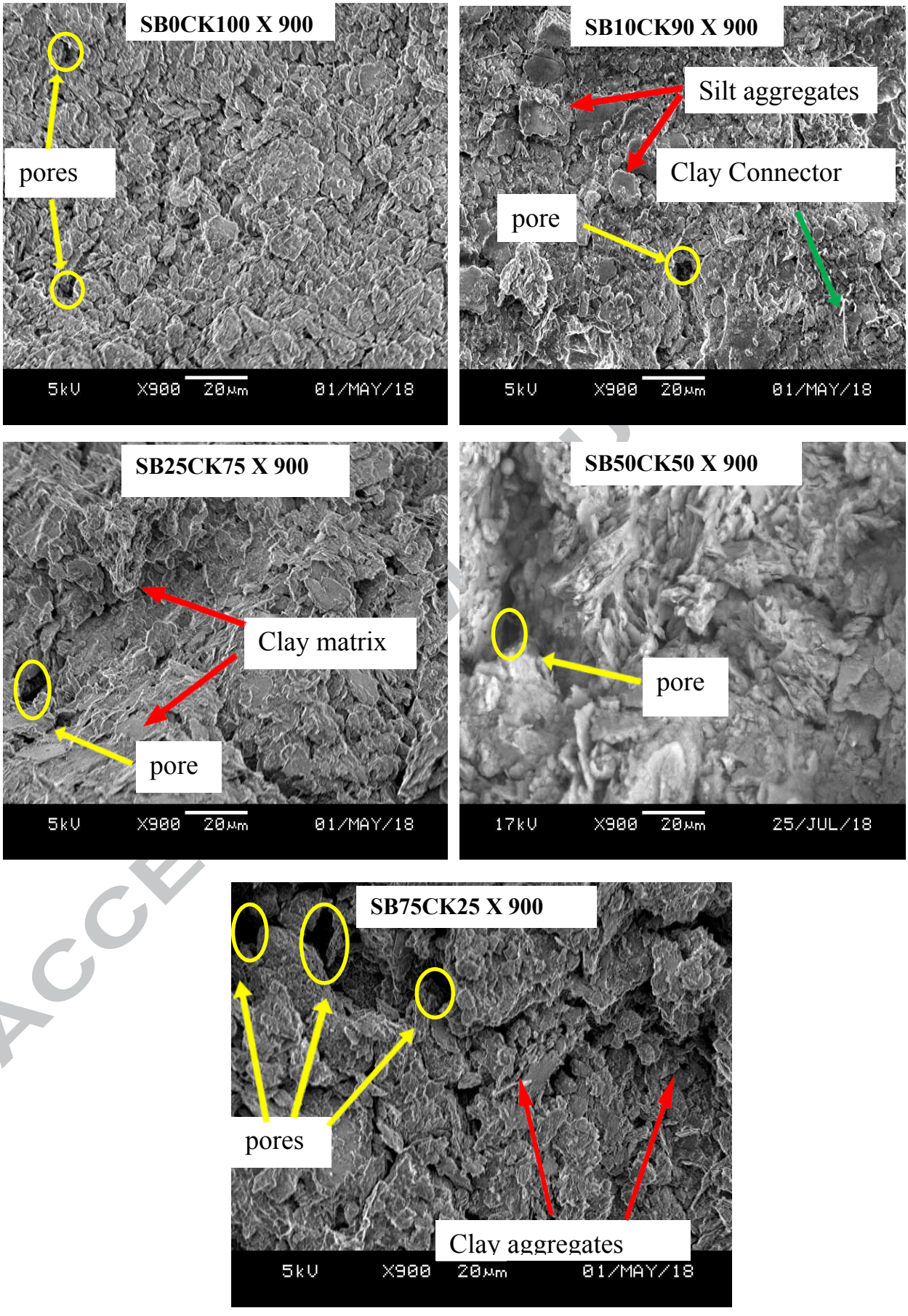

Fig. 4. Scanning electron micrograph (SEM)

Clay particle size grading

The clay particles were graded by the Laser Granulometer and the percentage sizes calculated by GRADISTAT program. This program uses Method of Moments in Microsoft Visual Basic programming language to calculate the grain size parameters [32]. The dry kaolin clay (SB0CK100) was determined as being uniformly-graded while the other clay mixtures (SB10CK90, SB25CK75, SB50CK50, SB75CK25) were adjudged as gap-graded as shown in Fig. 5. A precise fitting curve for particle-size distribution was achieved for the unimodal and bimodal particle size functions based on the equation proposed by Fredlund et al. [33].

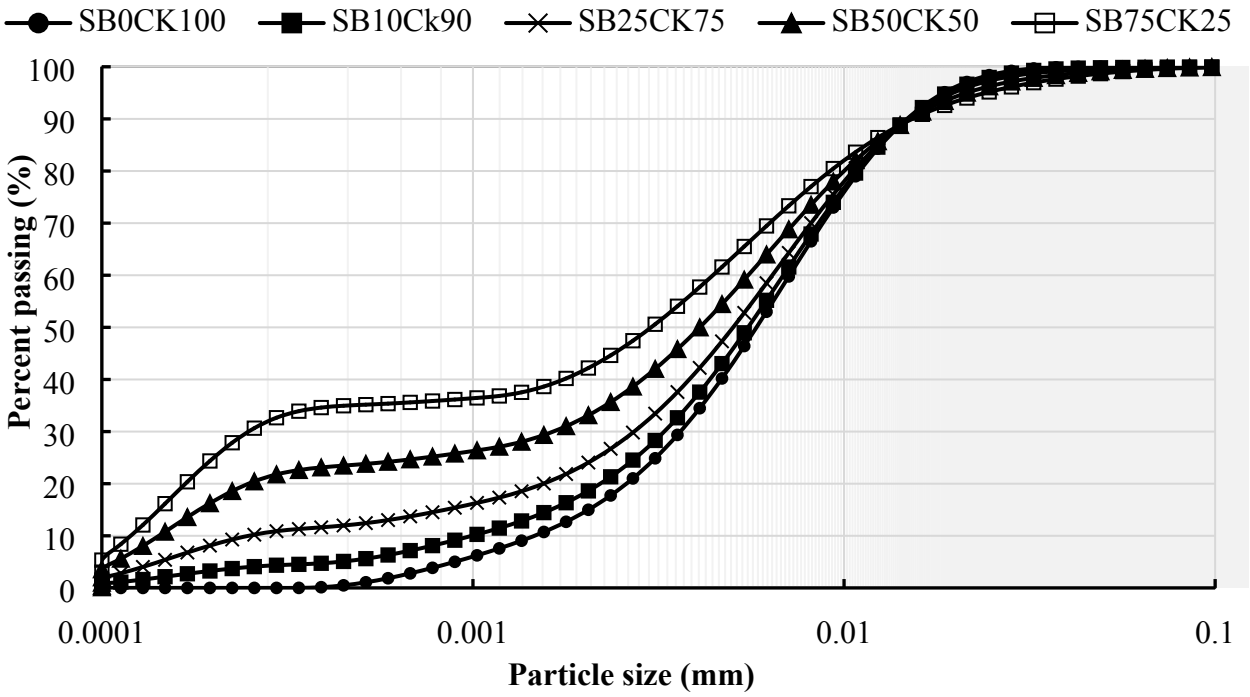

Fig. 5. Particle size distribution curve of the expansive clay samples.

Particle size analysis

Grain size analysis undertaken with the Malvern Mastersizer 2000 also enabled the determination of the specific surface area (SSA) of the clay particles. The Mastersizer calculates the SSA as the total area divide by the total weight Eq. 6 based on the assumption that the particles are both non-porous and spherical in shape [24].

$$SSA = \frac{6\sum\frac{V_i}{d_i}}{p\sum V_i} = \frac{6}{pD} \qquad \text{Eq. 6}$$

Where:

V_i = relative volume in class *i*

d_i = mean class diameter *i*

p = particle density

D = surface weighted mean (or surface area moment mean diameter or sauter mean)

Fig. 6 presents some relevant statistics from the particle-size analysis. A gradual reduction in the median of particle sizes, mean particle sizes of each whole sample and the effective size particles (D_{10} sizes) towards the finer fractions as the amount of montmorillonite increases could be observed. The median of the particle distribution fluctuates around 8μm which corresponds to 'medium silt' size particles (6-20μm). The highest of the mean particle size distribution as observed for SB0CK100 is about 8.2μm. This value reduces by approximately 67% as the percentage of the sodium bentonite increases to 75%. Meanwhile, the effective size for all the clays remains within the clay region (<2μm). Is it interesting to note as would be shown subsequently that the clay-sized particles seem to have more influence on the swell behaviour of the expansive clays.

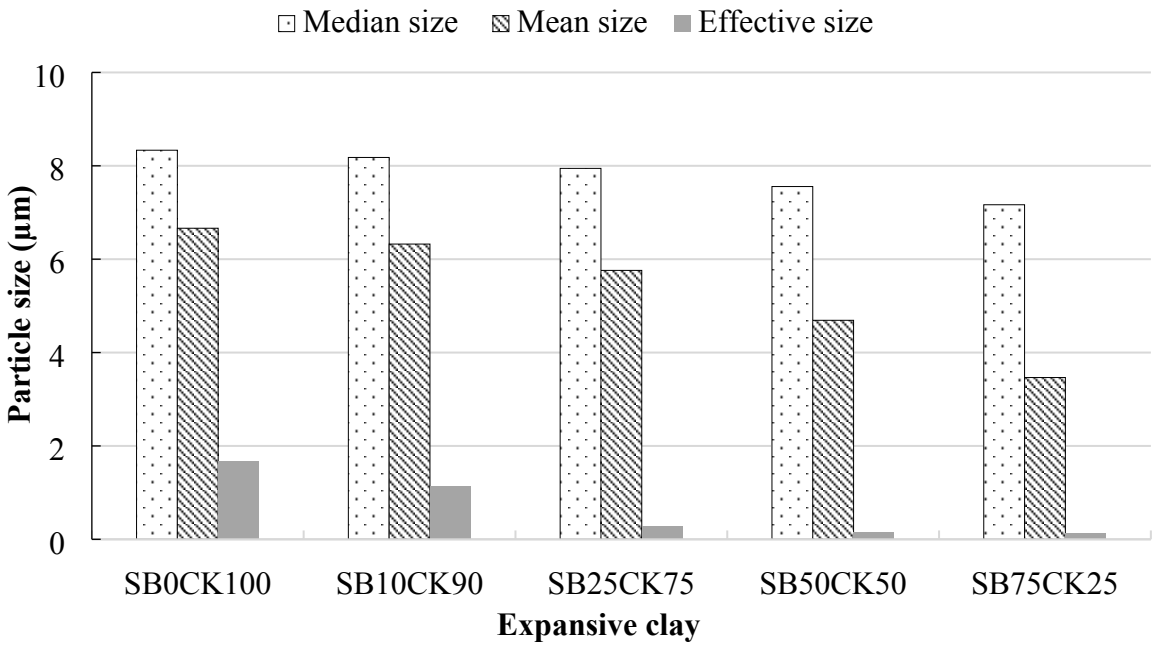

Fig. 6. Expansive clay particle size statistics.

Correlation of particle size with clay properties

Several researchers have attempted to provide a mere direct correlation of the clay-sized fraction (<2μm) of soils with swell potential and other soil properties [7,34,35]. However, in this research, the particle distribution curve of Fig 5 is used to critically examine the various size particles in a given clay soil sample and to demonstrate the effect of the particles on the factors that influence swell behaviour such as the specific surface area (SSA), plasticity index (PI) and activity (A) of the expansive clays. In order to execute this, the mean sizes of each individual fractions contained in the samples and the mean particle size of each sample considered as a whole both determined by the Malvern Mastersizer 2000 are considered. The particle fractions derived from the GRADISTAT are categorized into size classes [25] as shown in Table 3. Values of the mean sizes of the individual fractions and the mean size (henceforth referred to as d_p) of each whole sample are given in Table 4 which also includes, as well as Table 5, regression analyses performed to determine the relationship between the mean sizes (dependent variables) and the soil properties (PI, SSA and A).

Revised with marked changes

Table 3
Expansive clay size class fractions.

Soil fraction	Designation	Size range (μm)
Clay	C	0-2
Very fine silt	VFS	2-4
Fine silt	FS	4-8
Medium silt	MS	8-16
Coarse silt	CS	16-31
Very coarse silt	VCS	31-63

Table 4
Expansive clay particle sizes and soil properties.

Clay	Mean sizes							Soil Properties		
	Dependent variable							Independent variable		
	C	VFS	FS	MS	CS	VCS	d_p	PI	SSA	A
	μm							(%)	$(m^2)/g$	-
SB0CK100	1.03	2.059	4.305	9.089	18.94	37.8	6.663	14	1.7	0.67
SB10CK90	0.936	3.084	6.09	11.44	21.42	44.49	6.324	48	1.75	1.92
SB25CK75	0.69	3.079	5.98	11.43	21.58	42.18	5.76	82	6.03	2.73
SB50CK50	0.475	3.07	5.951	11.43	21.89	43.74	4.691	102	10.35	2.76
SB75CK25	0.357	3.059	5.91	11.42	22.28	44.54	3.465	191	14.68	4.06

Table 5
Regression analysis result.

Dependent variable	Regression Equation	R^2	F	*p*-value
C	0.973PI – 1.233SSA – 0.754A	0.99	308.25	0.042
VFS	-1.829PI – 0.204SSA + 2.722A	0.92	3.80	0.357
FS	-1.772PI – 0.343SSA + 2.752A	0.90	3.00	0.396
MS	-1.800PI – 0.192SSA + 2.692A	0.92	3.76	0.358
CS	-1.249PI +0.011SSA + 2.102A	0.94	4.89	0.318
VCS	-0.419PI – 0.632SSA + 1.749A	0.73	0.921	0.626
d_p	-0.528PI – 0.622SSA + 0.153A	0.99	44.88	0.109

All the mean size classes considered in the analysis seem to give much higher values of the coefficient of determination R^2 when correlated with the PI, SSA and A (Table 5). However, the regression analyses result also show that the only statistically significant correlation (*p*-value) considered within 95% confidence interval occurs between the mean size class involving the clay fractions, C and the predictor or independent variables. Hence, it could be said that the presence of the clay-sized particles in a clay samples could potentially affect the behaviour of expansive clay samples in swell given their strong correlation with the PI, SSA and A. Also, the approach presented herein regarding the relationship between the mean sizes of the representative clay fractions and the investigated soil properties appears relatively reasonable in describing the effect of clay fractions on swell. In the sections following, both the mean clay sizes and mean sizes of each whole samples are further compared.

Clay pore characteristics

An approach adopted from published literatures is utilized to determine the sizes of pores in the clay samples. The mean pore diameter (d_m) which is calculated for various particle geometries and fabrics in terms of the specific surface area (SSA) and void ratio e, is adopted for the determination of the average size pores in the clay samples [36]. By applying this theory, it is considered that the volume of voids is evenly distributed around the clay particles as a "void layer" of thickness, t. Then the distance between particles, $d_m = 2t$ void is taken as an estimate of the mean or average pore diameter as follows:

$$d_m = \frac{2e}{SSA \times \rho_m} \qquad \text{Eq. 7}$$

Where:

e	=	void ratio,
SSA	=	specific surface area (m2/ g),
ρ_m	=	mass density of the clay mineral (kg/m3)
d_m	=	mean pore diameter

The following assumptions are made in using Eq. 7

- The clay particles are round in shape and with parallel stacking arrangement.
- The compacted samples consist of dispersed fabrics or structure

Pore and particle size effect on swell

The swell behaviour of the expansive clays in this research is related to the following terms: mean pore diameter (d_m), mean particle diameter (d_p), mean clay diameter (d_{clay}) and the matric suction values.

Void ratio

The void ratio, e_f that corresponds to the final swell values of the clays (Fig. 2) is used to evaluate the mean diameter of the pores at maximum swell. According to Eq. 7 therefore, the mean of the maximum size of pore (d_m) at the end of the swell process (i.e at equilibrium) represents or describes the swell given that the final void ratio e_f at that point is used in the equation. The relationship between important clay soil swell properties (i.e. PI, SSA and A) and the particle sizes as demonstrated earlier revealed the potential significant contribution the mean particle fractions and the clay fraction could have on the overall swell behaviour of clays. Hence, the d_m and the d_{clay} are used to explain the swell characteristics of the expansive clays. The relationship presented in Fig. 7 and Fig. 8 depicting the variation of d_m with d_p and d_{clay} respectively, shows that despite an increase in the void ratio as the montmorillonite increases (Fig. 2.), the mean pore size tends to reduce. This explains why the permeability of the samples seems to reduce as the amount of montmorillonite increases as earlier observed (Fig. 3.). This is also the reason clays with high amounts of montmorillonite take much longer to reach the equilibrium swell. A strong relationship between the d_m and d_p is also noticed even though the mean clay diameter (d_{clay}) seems to produce a higher correlation than the mean particle size (d_p) which represents the entire soil samples. This does clearly validates the dependence of swell on the clay fractions in the samples [7,34,35]. Furthermore, the model Eq. 8 and Eq. 9 given in terms of the d_m, d_p and d_{clay} demonstrates that knowledge of either the average size of particle of the whole soil sample or the average size of the clay fraction (d_{clay}) in a soil sample can enable a direct determination of the average pore sizes (d_m) and an indirect evaluation of the final void ratio at maximum swell respectively.

Revised with marked changes

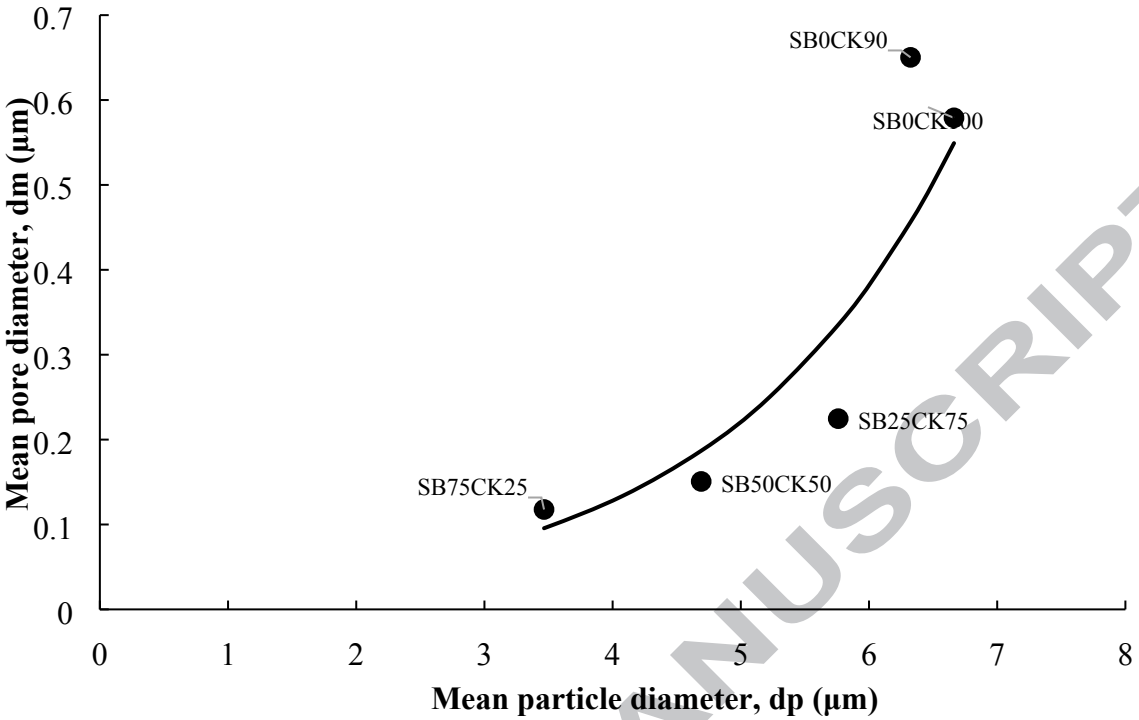

Fig. 7. Variation of d_m with d_p for the clay samples at maximum swell.

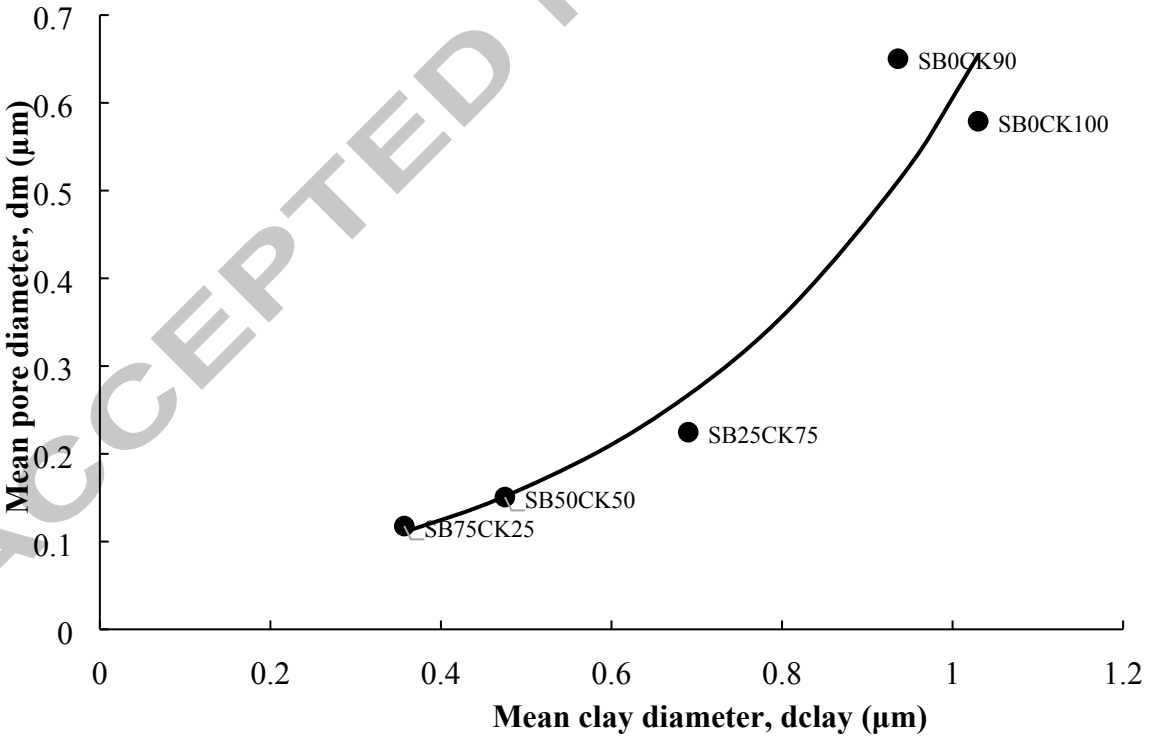

Fig. 8. Variation of d_m with d_{clay} for the clay samples at maximum swell.

$$d_m = 0.0144e^{0.55d_p} \qquad R = 0.85 \qquad \text{Eq. 8}$$

$$d_m = 0.0434e^{2.63d_{clay}} \quad R = 0.96 \qquad \text{Eq. 9}$$

Verification of the pore and particle size approach

Pedarla et al. [17] attempted an evaluation of the swell characteristics of eight natural expansive clays by relying on the pore size distribution and the SSA of the soils. They used a hypothetical parameter known as the total surface area ratio (TSAR) in the estimation of swell. TSAR was defined as the ratio of the total surface area (TSA) derived from clay fraction in the soils to the total pore surface area (TPA). Both the TSA and the TPA were analytically derived from the measurements using the EGME and the MIP methods. Table 6 presents the engineering characteristics of the clays used by the authors.

Table 6
Properties of the tested soils by Pedarla et al. [17].

Soil	PI	Vertical swell strain (%)
Keller	11	7.9
Oklahoma	21	4.8
Anthem	27	5.8
San Diego	28	4.4
Burleson	37	8.8
Colorado	42	12.0
San Antonio	43	10.2

Variation of the TSAR with the swell potential of the specimens is shown in Fig. 9 including the mean clay ratio (MCR) defined as the ratio of the mean clay diameter (d_{clay}) to the mean pore diameter (d_m) determined from this research. The X-axis of Fig. 9 combines the TSAR and the mean clay ratio (MCR). The TSAR and the MCR are evaluated at the initial soil placement conditions. As could be observed, the present concept from this research relying on the mean sizes of the particles and pores is in agreement with the model proposed by Pedarla et al. [17] and does possess a good relationship with the swell potential. The slight variation in both curves could be attributed to the difference in the soil properties used and loading conditions. However, irrespective of the contrast in methods used, it could be said that the concept presented in this research can be relied upon to describe swell properties of clays.

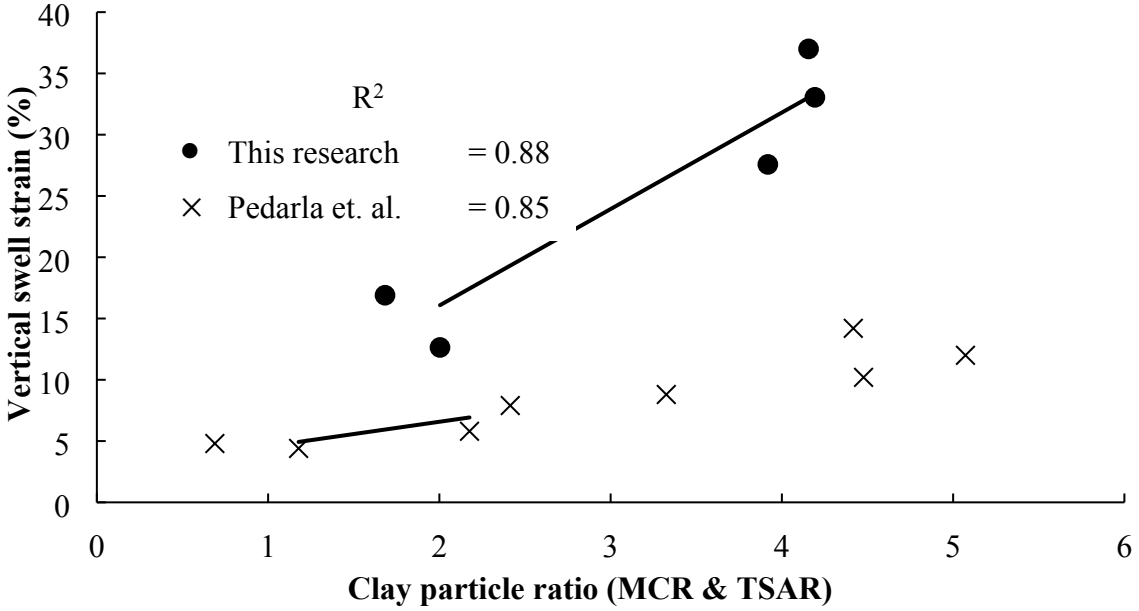

Fig. 9. Validation of approach based on the dependence of predicted swell on pore and particle sizes.

Suction

Fig. 10 and Fig. 11 show the variation of d_m at maximum swell with the suction values at initial condition and at air entry. It is obvious that the pores decrease in size with an increase in matric suction as the percentage of montmorillonite increases in the clay samples. This phenomenon verifies the claim that suction values are typically higher when the sizes of the voids are smaller. Since void ratio is a term used in the expression of d_m, Fig. 10 and Fig. 11 seem to be in agreement with the claims made earlier (Fig. 7 and Fig. 8) showing that despite an increase in the void ratio at maximum swell, the pore sizes seem to reduce as the amount of montmorillonite increases. Furthermore, it can be seen that highly plastic soils tend to possess higher AEV suction due to smaller pore sizes as compared to soils of low plasticity [33]. By using the capillary phenomenon, it is known that during the wetting process, water seems to rise higher (high head or energy or suction) through a cylindrical-sized tube having smaller diameter than one with higher diameter by dispelling the remaining air in the tube. Hence, the capacity of the clays with higher plasticity and smaller diameter to retain water and then swell is more than those of clays possessing low plasticity and larger pore spaces. It can be observed that the clays at their initial suction condition seem to show a stronger relationship with the d_m at maximum swell, as compared to the AEV of suction. This validates the claims by several authors [21,37,38], that the initial matric suction values can be relied upon for the determination of the swell characteristics of clays.

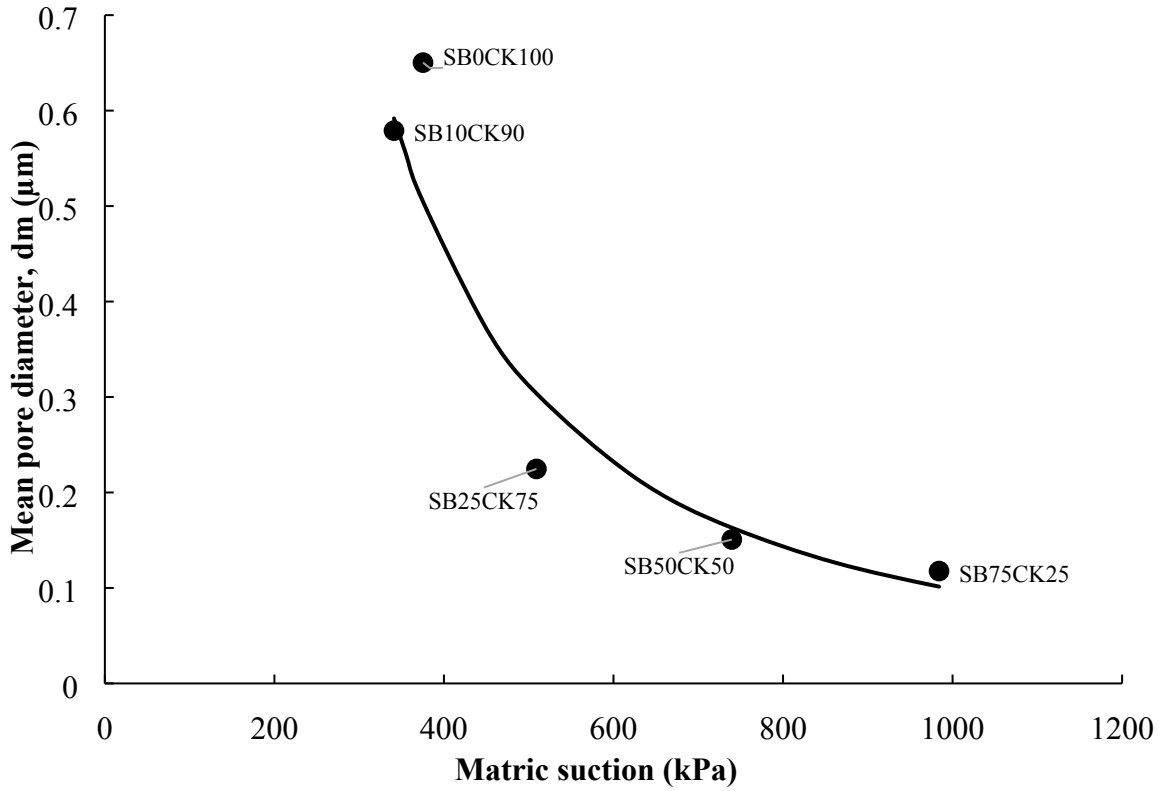

Fig. 10. Relationship between d_m at maximum swell and initial suction.

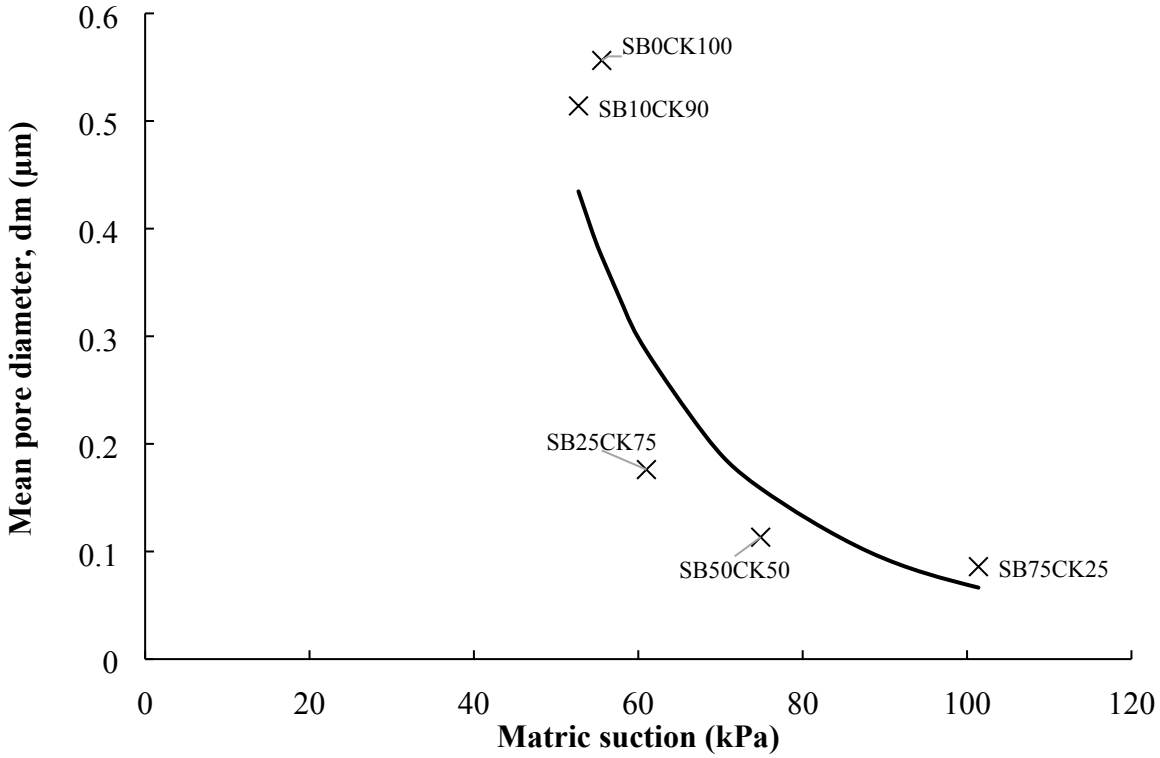

Fig. 11. Relationship between d_m at maximum swell and air-entry suction (AEV).

Conclusions

This note has attempted to describe and evaluate the complex swelling mechanism of five expansive clays having varying montmorillonite mineral content with the following conclusions:

- An approach using the laser technology and GRADISTAT to determine mean particle size fractions and relating such with the SSA, PI and A through a multiple regression analysis showed the strong dependence of clay-sized particles on swell within 95% confidence interval.

- Relationship between the mean pore sizes and the mean clay sizes demonstrated the presence of reduced pore sizes and increased void ratio at maximum swell as the plasticity increases and further provided satisfactory estimates of swell strain with coefficient of determination R^2 exceeding 0.90. This approach also explained why it takes longer for a highly compacted montmorillonite-rich clay to reach its maximum swell potential.

- The model relationship involving the mean pore sizes at both the initial suction and AEV does sheds more light on the capillary phenomenon which shows the capacity of the clays with higher plasticity and smaller diameter to retain water and then swell as compared to clays possessing low plasticity and larger pore spaces. Satisfactory coefficient of determination values indicating the importance of suction conditions in the description of swell properties was achieved.

- Overall, it is clear that the swell-strain formulation conceived in this research provides a rather reasonable framework for the evaluation of swell hence highlighting the critical significance of the expansive clay's intrinsic microstructural properties and suction.

References

[1] Nelson JD, Miller DJ. Expansive soils: Problems and practice in foundation and pavement engineering. John Wiley & Sons, Inc; 1992.

[2] Nelson JD, Chao KCG, Overton DD, Nelson EJ. Foundation engineering for expansive soils 2015:416. doi:10.1016/B978-0-444-41393-2.50006-5.

[3] Abbey SJ, Ngambi S, Coakley E. Effect of cement and by-product material inclusion on plasticity of deep mixing improved soils. International Journal of Civil Engineering and Technology 2016;7:265–74.

[4] Abbey SJ, Olubanwo AO. Strength and hydraulic conductivity of cement and by-product cementitious materials improved soil. International Journal of Applied Engineering Research 2018;13:8684–94.

[5] Abbey SJ, Ng'ambi S, Ganjian E. Development of strength models for prediction of unconfined compressive strength of cement/by-product material improved soils. Geotechnical Testing Journal 2017;40:928–35. doi:10.1520/GTJ20160138.

[6] Rahgozar MA, Saberian M, Li J. Soil stabilization with non-conventional eco-friendly agricultural waste materials: An experimental study. Transportation Geotechnics 2018;14:52–60. doi:10.1016/j.trgeo.2017.09.004.

[7] Seed HB, Woodward RJ, Lundgren R. Prediction of swelling potential for compacted clays. Journal of the Soil Mechanics and Foundations Division 1962;88:53–87.

[8] Chen FH. Foundations on expansive soils. Elsevier; 1975.

[9] Nalbantoğlu Z. Effectiveness of class C fly ash as an expansive soil stabilizer. Construction and Building Materials 2004;18:377–81.

[10] Seco A, Ramírez F, Miqueleiz L, García B. Stabilization of expansive soils for use in construction. Applied Clay Science 2011;51:348–52.

[11] Eyo EU, Ngambi S, Abbey SJ. Investigative study of behaviour of treated expansive soil using empirical correlations. International Foundation Congress and Equipment Expo 5-10 March, Orlando, Florida: 2018, p. 373–84.

[12] Eyo EU, Ngambi S, Abbey SJ. Investigative modelling of behaviour of expansive soils improved using soil mixing technique. International Journal of Applied Engineering Research 2017;12:3828–36.

[13] Puppala AJ, Pedarla A, Hoyos LR, Zapata CE, Bheemasetti T V. A semi-empirical swell prediction model formulated from "clay mineralogy and unsaturated soil" properties. Engineering Geology 2016;200:114–21.

[14] Punthutaecha K, Puppala AJ, Vanapalli SK, Inyang H. Volume change behaviors of expansive soils stabilized with recycled ashes and fibers. Journal of Materials in Civil Engineering 2006;18:616–7.

[15] Likos WJ, Wayllace A. Porosity evolution of free and confined bentonites

during interlayer hydration. Clays and Clay Minerals 2010;58:399–414. doi:10.1346/CCMN.2010.0580310.

[16] Chittoori B, Puppala AJ. Quantitative estimation of clay mineralogy in fine-grained soils. Journal of Geotechnical and Geoenviromental Engineering 2011;137:997–1008. doi:10.1061/(ASCE)GT.1943-5606.0000521.

[17] Pedarla A, Puppala AJ, Hoyos LR, Chittoori B. Evaluation of swell behavior of expansive clays from internal specific surface and pore size distribution. Journal of Geotechnical and Geoenvironmental Engineering 2016;142:04015080. doi:10.1061/(ASCE)GT.1943-5606.0001412.

[18] Villar MV, Lloret A. Influence of dry density and water content on the swelling of a compacted bentonite. Applied Clay Science 2008;39:38–49. doi:10.1016/j.clay.2007.04.007.

[19] Alonso EE, Vaunat J, Gens A. Modelling the mechanical behaviour of expansive clays. Engineering Geology 1999;54:173–83. doi:10.1016/S0013-7952(99)00079-4.

[20] Castellanos E, Villar M V., Romero E, Lloret A, Gens A. Chemical impact on the hydro-mechanical behaviour of high-density FEBEX bentonite. Physics and Chemistry of the Earth 2008;33:516–26. doi:10.1016/j.pce.2008.10.056.

[21] Erzin Y, Erol O. Swell pressure prediction by suction methods. Engineering Geology 2007;92:133–45. doi:10.1016/j.enggeo.2007.04.002.

[22] Horpibulsuk S, Yangsukkaseam N, Chinkulkijniwat A, Du YJ. Compressibility and permeability of Bangkok clay compared with kaolinite and bentonite. Applied Clay Science 2011;52:150–9. doi:10.1016/j.clay.2011.02.014.

[23] Romero E, Vecchia D, Jommi C. An insight into the water retention properties of compacted clayey soils. Géotechnique 2011;61:313–28. doi:10.1680/geot.2011.61.4.313.

[24] Malvern. Mastersizer 2000 essentials user manual 2007.

[25] Blott S, Pye K. A grain size distribution and staistics package for the analysis of unconsolidated sediments. Earth Surface Processes and Landforms 2000:1237–48.

[26] Leong EC, He L, Rahardjo H. Factors affecting the filter paper method for total and matric suction measurements. Geotechnical Special Publication 2002;25:1–12. doi:10.1520/GTJ11094J.

[27] Gvirtzman H, Roberts P V. Pore scale spatial analysis of two immiscible fluids in porous media. Water Resources Research 1991;27:1165–76. doi:10.1029/91WR00303.

[28] Fraser HJ. Systematic packing of spheres with particular relation to porosity and permeability 1935;XLIII.

[29] Al-Swaidani A, Hammoud I, Meziab A. Effect of adding natural pozzolana on geotechnical properties of lime-stabilized clayey soil.

Journal of Rock Mechanics and Geotechnical Engineering 2016;8:714–25. doi:10.1016/j.jrmge.2016.04.002.

[30] Al-Rawas AA, Hago AW, Al-Sarmi H. Effect of lime, cement and sarooj (artificial pozzolan) on the swelling potential of an expansive soil from Oman. Building and Environment 2005;40:681–7.

[31] Latifi N, Rashid ASA, Siddiqua S, Horpibulsuk S. Micro-structural analysis of strength development in low- and high swelling clays stabilized with magnesium chloride solution - A green soil stabilizer. Applied Clay Science 2015;118:195–206. doi:10.1016/j.clay.2015.10.001.

[32] Krumbein WC, Pettijohn FJ. Manual of sedimentary petrography 1938.

[33] Fredlund DG, Xing A. Equations for the soil-water characteristic curve. Canadian Geotechnical Journal 1994;31:521–32.

[34] Ranganatham BV, Satyanarayana B. A rational method of predicting swelling potential for compacted expansive clays. Proceeding of the 6th ICSMFE 1965:92–96.

[35] Basma AA. Prediction of Expansion Degree for Natural Compacted Clays. ASTM Technical Note 1993:542–9.

[36] Phadnis HS, Santamarina JC. Bacteria in sediments: pore size effects. Géotechnique Letters 2011:91–3. doi:10.1680/geolett.11.00008.

[37] Rao BH, Venkataramana K, Singh DN. Studies on the determination of swelling properties of soils from suction measurements. Canadian Geotechnical Journal 2011;48:375–87.

[38] Zhan L, Chen P, Ng CWW. Effect of suction change on water content and total volume of an expansive clay. Journal of Zhejiang University-Science A 2007;8:699–706. doi:10.1631/jzus.2007.A0699.